Mirror Smooth Surfaces and Repair of Weld Defects in Superconducting RF Cavities by Mechanical Polishing

CA Cooper and LD Cooley

Fermi National Accelerator Laboratory, PO Box 500, Batavia, IL 60510, USA

E-mail: ccooper@fnal.gov

Abstract
Mechanical techniques for polishing the inside surface of niobium superconducting radio-frequency (SRF) cavities have been systematically explored. By extending known techniques to fine polishing, mirror-like finishes were produced, with < 15 nm RMS roughness over 1 mm^2 scan area. This is an order of magnitude less than the typical roughness produced by niobium cavity electropolishing, which could be important for reduction of field emission and as preparation for high-quality films or coatings. The extended mechanical polishing (XMP) process was applied to several SRF cavities which exhibited equator weld defects that caused quench at < 20 MV m^{-1} and were not improved by further electropolishing. Cavity optical inspection equipment verified the complete removal of these defects, and minor acid processing, which dulled the mirror finish, restored performance of the defective cells to the high gradients and quality factors measured in adjacent cells when tested with other harmonics. This innate repair feature of XMP could be used to increase manufacturing yield. Excellent superconducting properties resulted after initial process optimization, with quality factor Q of 3×10^{10} and accelerating gradient of 43 MV m^{-1} being attained for a single-cell TESLA cavity, which are both close to practical limits. Several repaired 9-cell cavities also attained $Q > 8 \times 10^9$ at 35 MV m^{-1}, which is the specification for the International Linear Collider. Future optimization of the process and pathways to eliminate requirements for acid processing are also discussed.

(Some figures in this article are in colour only in the electronic version)

1. Introduction

Niobium superconducting radio-frequency (SRF) resonating cavities are an enabling technology for efficient particle accelerators. They are central to physics machines that produce high-energy and high-intensity beams, and they enable other applications such as next-generation light sources, sub-critical nuclear reactors and spent fuel remediation, medical isotope production, emissions reduction, and screening for defense and security [1]. Important metrics of SRF cavity technology are manufacturing yield, the quality factor Q, and the accelerating electric field E_{Acc} to which high values of Q can be sustained [2]. These quantities drive cost and performance factors related to cryogenics, beam energy, machine length, and other aspects.

The present state of cavity fabrication and processing art places emphasis on attaining a smooth surface because high Q can be maintained to high E_{Max} as the surface roughness is decreased [3,4]. When operated in the usual mode that aligns the electric field with the cavity axis to accelerate a particle beam, magnetic fields align with the cavity surface and are highest near the cell equator. The high magnetic fields seen near the cell equators can cause flux penetration and a local breakdown in the superconducting state that eventually leads to global quenching of the cavity. Onset of flux penetration can be delayed by superheating the Meissner state, up to a field substantially higher than the lower critical field and slightly higher than the niobium thermodynamic critical field [5, 6]. However, sharp points, edges, ridges, and other topographical features where the geometry imparts a local enhancement of the magnetic field have been proposed as sources of local breakdown of the superheating state [7]. This may explain why smooth surfaces perform better than rough surfaces at high E_{Acc} [8-10]. It would be interesting, therefore, to explore how extremely smooth surfaces might perform. Also, ideally smooth surfaces could permit a better evaluation of the impact of contamination on cavity performance, in particular the effects of dislocations and defects created by forming, and hydrogen and oxygen taken up by the metal during processing. From a more practical point of view, surface polishing techniques that also prevent or reduce sub-surface contamination are highly desirable.

Electropolishing (EP) is presently the preferred route for preparing the final cavity interior surface. A well-controlled EP process can produce a typical average roughness R_A of approximately 0.1 µm for a 1 mm × 1 mm area scan using a profilometer [3, 4]. Here, distinction is made between polishing in 2 steps, the first being a "bulk" removal of 100 to 150 µm of metal, and the second being a "final" or "light" removal of 20 to 40 µm of metal. The "bulk" removal step appears to be less important for the final properties, where EP, buffered chemical polishing (BCP), and mechanical abrasive techniques can each be used to obtain good results when "light" EP is the second step [XFEL]. The "light" EP often occurs at lower temperature and under tighter control than the EP parameters used for the bulk removal step, thereby optimizing the leveling process. While EP is now managed on an industrial scale, it has several drawbacks. The electrolyte that is typically used, 9 parts by volume 98% concentrated sulfuric acid and 1 part 49% concentrated hydrofluoric acid [16], is toxic and requires extensive facilities, training, and operation protocols. Spent acid must be disposed of as a hazardous toxin. Sulfur byproducts can form and deposit on the surface, potentially limiting cavity performance [17,18]. In addition, the complexity of the EP process can make it difficult to control the fluorine ion diffusion [18]. Nonetheless, EP is the established processing baseline for the International Linear Collider (ILC), and it has produced excellent performance in scores of SRF cavities [Ginsburg].

A particular problem that EP cannot address is the removal of pits near the equator welds. Such pitting has significant negative consequences for SRF cavities, often limiting performance to < 20 MV m^{-1}. (Values of Q and E_{Acc} throughout this paper were obtained at 2.0 K, as is customary for SRF cavity tests). It is not clear at present whether pits are a result of conditions resident in the material, flaws of the material preparation prior to welding, flaws in the welding process itself, flaws in the EP process, or a combination of these [19]. Because the layer that controls fluorine ion diffusion is ~10 µm in scale [20], whereas many weld pits are > 100 µm in size, the basic mechanisms of electropolishing are not useful for removing pits. Indeed, work on coupons shows that the profile of a pit is retained while its small-scale features are gradually smoothed by successive EP treatments [21].

This article describes experiments to use mechanical polishing to achieve smoother surfaces and repair cavity defects. At its utmost limit, the procedures described herein achieved a mirror-smooth surface finish with R_A < 15 nm. The general technique is derived from centrifugal barrel polishing (CBP), which has been applied to SRF cavities previously [22,23] as a bulk removal stage prior to other chemical polishing. While CBP in this sense was also applied to the cavities reported here for the initial material removal steps that scrape away the equator weld bead and its defects, new techniques were innovated to achieve fine polishing by mechanical means with the same apparatus. This includes the use of novel media, which resulted in smoothing and polishing action more akin to the preparation of metallography samples with atomically flat surfaces. Although dependence upon acid has not yet been completely removed, the extended mechanical polishing (XMP) steps are friendly to the environment and worker

safety. The creation of mirror-smooth surfaces without chemical contamination is an important enabling step for production of thin films, such as niobium films on copper [Krish, Benvenuti], or new SRF materials, such as Nb_3Sn [Wuppertahl, Posen], MgB_2 [Tajima], or multilayers [Gurevich]. The ability to repair pits should correlate to higher manufacturing yields and cheaper costs for linear accelerators.

2. Description of the extended mechanical polishing process

Extended mechanical polishing of single-cell and 9-cell SRF cavities used a machine custom built for this purpose by Mass Finishing Inc. [25]. The machine was designed accelerate a slurry media by approximately 10g against the inner cavity surface. Cavities were secured in buckets, where each bucket rotated around the central shaft at up to 115 rpm, while at the same time each bucket counter-rotated around its own axis at the same rate. Since polishing was done with the cavity axis horizontal, counter-rotation evenly distributed any effect of gravity. Counter-rotation also increased the viscous shear of the slurry along the cavity surface, which was found to improve the polishing action. The cavities were filled 50% by volume with media and capped for each step. Special components were designed to protect the input and higher-order mode couplers from the media. The end caps and other components were made from the same type of niobium as the cavities. The cavities were rinsed with water between polishing steps.

Approximately 20 different types of media were studied initially. A subset of 5 steps, described below, was found to be effective for niobium cavities. The XMP process consisted of one bulk material removal step and up to 4 polishing steps, all conducted at ambient temperature. The first 2 steps followed earlier CBP work: In the first step, 9 mm × 9 mm KM ceramic angle cut triangle media (a solid ceramic), purchased from Kramer Industries, Inc., was spun inside the cavity to remove approximately 80 μm of material at a removal rate of 11 μm hr^{-1}. This step intended to scrape away the equatorial weld bead. The second step ran for 12 hours at a material removal rate of 3 μm hr^{-1} using 12.5 mm RG-22 cones (a composite of ceramic and binder) from Mass Finishng, Inc. Both steps used enough de-ionized (DI) water to just cover the media and a surfactant called TS Compound provided by Mass Finishing, Inc. (1 TS Compound : 40 parts water).

The final 3 steps diverged from previous CBP work and followed metallurgical sample preparation guidelines. They all used 4 mm cubic hardwood blocks (Raytech Metal Finishing, part number 41-363) to hold various polishing slurries. The blocks were found to be superior to other fibrous organic and inorganic media. The third step used 400 mesh alumina powder, the fourth step 800 mesh alumina powder (both from Kramer Industries, Inc), and the final step used 40 nm colloidal silica (Allied High Tech Products Inc., part number 180-25000). The alumina was mixed at 50 to 100 g alumina per liter of solution. The wood blocks were soaked in the alumina-water and colloidal silica for 12 hours before use. Processing times were 15 hrs for step 3, 20 hrs for step 4, and 72 hrs for step 5. All of the cavities discussed herein were processed with the first 4 steps, and some were polished to step 5. Cavities that were polished to a mirror finish were subsequently given standard treatments including electropolishing, high-vacuum heat treatment at 800 °C, high-pressure rinse with ultrapure water, and assembly with couplers and fittings in a class 10 clean room.

3. Qualitative and quantitative evaluation of the surface finish

Cavities were not cut apart to expose the actual polished surface. Instead, the surface roughness of the niobium end caps was measured using a KLA-Tencor P-16 Stylus-Type surface profilometer with a 0.1 micron diameter tip. The force on the end cap is not as much and not in the same direction as at the cavity equator. However, the visual appearance of the end caps was comparable to that of the rest of the cavity interior. At this time, the end caps are the most representative samples of the interior surface. Replicas [25] were not useful since the surface roughness was below the range intended for the compounds available.

Figure 1 shows the surface finish obtained by XMP compared to that obtained by a standard EP procedure. Pictures of the equatorial welds were taken by a special camera system [26] designed to access the cavity interior. This system has 20 μm resolution. In all pictures, the weld bead (WB) is approximately 10 mm wide and runs from top to bottom. Adjacent to the weld bead and running parallel to it on either side is a heat-affected zone (HAZ), which is approximately 15 mm wide. The material thickness is reduced prior to welding to control the thickness of the cosmetic under–bead, since the full-penetration weld is made from the outside of the cavity in a horizontal geometry. This standard machining step produces a fairly sharp demarcation at the edge of the HAZ also running parallel to the weld bead. Bulk niobium extends beyond this latter boundary. The entire weld, which runs circumferentially around the cavity equator, was scanned for each cavity. The pictures in Figure 1 represent 3° sections of the full 360° welds, and each is typical of the approximately 120 images acquired. The direction the media moves against the surface is parallel to the weld.

Figure 1(a), 1(b) and 1(c) are from the WB of single cell cavity TE1AES005. Figure 1a shows the cavity after the standard EP treatment. The individual grains are easily distinguishable, with shadowing evident at the grain boundaries. This is indicative of height differences between the grains. The WB, HAZ, and bulk regions can clearly be distinguished, and differences in grain morphology between these regions is also evident. Figure 1(b) is the exact same area as in figure 1(a), but after extended mechanical polishing to a mirror finish. It should be noted that the electropolished surface depicted in figure 1(a) was completely erased by the first 2 steps of mechanical polishing. The surface looks very homogeneous in figure 1(b), and no grain boundaries or demarcations of WB or HAZ are visible. There are tiny scratches running from top to the bottom of the picture that are approximately 20 μm wide. These marks are most likely left from the alumina in the next to last step or the wood blocks used in the final two polishing steps. Figure 1(c) shows the effect of 10 μm of electropolishing on the mirror finish. While grain boundaries reappear in the WB and HAZ, the top-to-bottom marks left by the media are mostly removed. The wide black bands running from top to bottom in figure 1(b) and 1(c) are actually reflections of the light-emitting diode array used for illumination by the camera system.

Even more dramatic, Figure 2 shows a picture of a single cell cavity and a nine cell cavity taken with a digital camera viewing through the end flange. The appearance of these cavities is impressive because of the mirror finish and the high number of reflections of light. The mirror finish makes the surface itself difficult to photograph because there are so few edges or other features to focus on. If Figure 2(a) is examined closely, an overhead crane can be seen in the reflection (the 2 orange rails). There is also the reflection from a piece of graph paper on the cavity, where the surface finish is smooth enough to distinguish the grid pattern distorted by the round geometry of the beam tube. Figure 2(b) shows a picture of a nine cell cavity that also has a mirror finish. Blue cellophane was placed in front of the light source to try to cut down on some of the reflection.

Figures 3 and 4 show the effect of each of the 5 different media on the surface of the niobium end plate used to cap the cavities during XMP. Figure 3 plots the RMS deviation (R_Q, S_Q) and arithmetic mean deviation (R_A, S_A) for the sample after each XMP step. S_Q and S_A are values for the entire 1 mm by 1 mm surface scan (3D values), while R_Q and R_A are values for 1 mm long lines extending across the scan area (2D values). The R_Q and R_A values are the average of 1000 lines spaced 1 μm apart. No error bars are shown because they lie within the data markers on the graph. All the parameters show the same general trend, with large decreases in values produced by the sequence from step 2, the first polishing step, to step 5, polishing with colloidal silica. The R_A is decreased finally to 14 nm and the S_A to 48 nm. These values are significantly less than the 0.1 μm R_A values typically obtained by EP [3,4]. The maximum peak height R_P, maximum valley depth, R_V, and total height $R_T = (R_P + R_V)$ are also useful 2D statistics to help characterize the effects of XMP on the surface. Figure 4 shows a plot of these values after each step along with S_T, the 3D total height of the surface. S_T decreased from 9.6 μm to 1.6 μm during polishing. However, since the plane of the sample is not flat, the profilometer algorithm probably over-estimates the final S_T value.

The most dramatic decrease in surface profilometry properties comes in the final step of polishing using 40 nm colloidal silica. It is thought that in this key step the polishing mechanism is changing from

micromachining to delamination [27]. During micromachining, media drags across the surface, embedding points into the surface. During delamination, smooth or flat edges of media adhere to the surface momentarily, then pull off small bits of the surface under the motion of the polishing media. Delamination has a lower risk of chips or pieces of the media breaking off and becoming embedded in the surface, so the final step leaves much less contamination. However, since the micromachining media consists of both points and flat edges, delaminating can actually begin at the micromachining stage, smearing metal over embedded grit and debris. The chemical affinity of the metal for the media affects this crossover. For example, it can also be seen in the surface profilometry data that the valleys are consistently deeper than the peaks are high. The reason for this is unclear, but it could be due to the nature of the polycrystalline niobium itself. The data also showed that step 3 was doing little or nothing to improve the surface, so it was removed from future runs with no apparent negative effects on cavity performance.

Taken as a whole, the qualitative and quantitative analyses of the cavity surface finish show a very dramatic improvement of the smoothness of the cavity produced by XMP as compared to EP. The surface finish was reproducible and the polishing process was predictable, with consistent roughness values emerging after a given stage of polishing. Robustness and consistency of process are very important to superconducting applications using cavities.

4. Repair of manufacturing defects

One of the motivations to develop the XMP process came from the possibility to repair large cavity defects such as pits or inclusions, while creating a homogenous surface suitable for light chemical polishing. This permits a repair step to be appended to the present industrial process as a means of improving production yield. A central problem with EP is its tendency to retain topographic profiles for features larger than a few tens of micrometers. This means that defects such as weld pits, which can be several hundred micrometers across and 10 to 100 μm deep, are not removed by bulk EP, even though the topography becomes smoother. For cavities that are limited by quench at such defects, repeated EP processing often does not repair this situation. On the other hand, the mechanical grinding action of CBP and the first steps of XMP completely remove such manufacturing defects. The fine polishing stages of XMP then conditions the surface for light EP. The ability to repair defects of up to 800 microns in size was demonstrated before on 9 cell cavity TB9AES006 using the XMP process [28]. The accelerating gradient of this cavity improved from 22 MV/m after processing with the standard EP technique to 36 MV/m after processing with the XMP technique.

In addition to being able to remove pits or voids, XMP can remove metal flakes and inclusions. These types of defects can also be resistant to EP. Figure 5 shows multiple pictures of 2 defective areas near the weld bead region of cavities RRCAT003. Figure 5(a) and 5(c) were acquired just after manufacturing with and before any chemical processing. Both pictures have a single nondescript black dot that is on the order of 1 mm in diameter. Figure 5(b) and 5(d) show the same areas as in 5(a) and 5(c), respectively, after bulk EP. The black feature appears to have not been affected by EP, and figure 5(d) in particular shows that there is a heavily etched "trench" around the location of the feature but little apparent effect on the inclusion itself. Since the forming die is made from aluminum, and aluminum is not affected by EP, it was concluded that this may be an aluminum flake, although confirmation of this hypothesis would require destruction of the cavity. Figure 5(e) shows the same area as 5(a) and (c) but after the XMP process. The surface is very homogeneous with no signs of the defect left behind.

The effect of XMP on the performance of RRCAT003 can be seen in Figure 6. Figure 6 shows a graph of the accelerating gradient of the cavity versus the quality for the cavity after baseline processing with electropolishing and after processing with XMP. At 2 K the accelerating gradient improved from 15 MV/m to 35 MV/m after the XMP process. At 1.8 K the cavity reached 40 MV/m after the XMP process. The XMP process in this instance demonstrates the ability to overcome some major manufacturing defects, which could not be repaired by electropolishing to yield a high performing cavity.

Figure 7(a) shows the surface of the 9-cell cavity TB9ACC015 after the cavity had received bulk EP as part of the standard cavity polishing regimen. An obvious defect is visible. This defect looks very similar to those shown from RRCAT003. After cold testing with this defect the cavity performed very poorly, reaching approximately 19 MV/m with a quench initiated in this cell by the defect. Subsequently, the first 4 steps of the extended mechanical polishing process were applied to remove 120 μm of metal, followed by 60 μm of EP. Figure 7(b) shows no sign of the pit at its earlier location. After mechanical polishing to an intermediate finish followed by EP the cavity reached 35 MV/m with a quality factor above 2×10^{10}. The quality factor, shown in Figure 8, showed little degradation with increasing gradient and was 1.4×10^{10} at 35 MV/m in fundamental mode, thus reaching the qualifying gradient for the International Linear Collider ($Q > 8 \times 10^9$ at 35 MV m^{-1}).

Subsequent to these successful repair results, several other cavities have been given similar repair treatments, and in all cases improvement of the cavity performance has been noted. . In one case, where the weld showed porosity, new defects appeared at different locations, consistent with the possibility that mechanical polishing could uncover defects buried beneath the niobium surface. However, in cavities with high-quality welds, so far there has not been an instance where a new defect emerged. Cavity repair by XMP thus appears to be a viable procedure for improving the production yield of high-gradient cavities for accelerators

5. Discussion

In general, all SRF cavities require some removal of material from their interiors due to the metallurgical damage introduced by forming and welding, and due to contamination that penetrates the surface. It is well known that Q and E_{Acc} increase with increasing amount of removed metal, up to a point where the damaged material is removed and the uncovered pristine metal provides the best superconducting properties. Although the particular nature of the damage and contaminants has been debated widely for 4 decades [2], all of the cavity processing techniques seek a common goal of removing material and leaving behind a clean, smooth surface. None of the processes is perfect, and post processing steps, such as baking in high-vacuum ovens, "light" chemical processing, and high-pressure rinsing, are always required to remove artifacts introduced by the bulk material removal technique. Thus, any SRF cavity process must strike a balance between efficiently removing the starting material damage and minimizing the introduction of new factors that reduce superconducting performance.

The successful repair of cavity defects without generating new defects is an important advance. Studies of the ILC cavity production showed that 20% of cavities produced prior to 2010 suffered from significant defects that limited performance to < 20 MV m^{-1}, and as high as 50% did not meet the ILC specification after repeated processing [Geng]. While manufacturing has greatly improved [Ginsburg], present estimations assume that only 60% of cavities would meet or exceed the specification after the first processing pass today. Cavity test data commonly indicates that specific flaws impose quench limits on cavities that fail, and many times these flaws persist after second EP steps. This may be because chemical processes remove material based on topography (EP) and crystallographic orientation (BCP) of the underlying metal, so that flaws in the metal alter the basic chemical processes. By contrast, mechanical polishing is largely governed by factors not dependent on the metal, such as force, viscosity, and media size and shape. This permits mechanical techniques to overcome material flaws in ways chemical processing cannot. The repair results discussed here suggest that a high first-pass success rate could be achieved when XMP is coupled with a final light EP because the polishing action removes the local flaws that limit cavity accelerating gradient. This will be evaluated in processing trials.

The mirror-smooth surface finish should be useful, and perhaps enabling, for coating the cavity interior with a thin film or coating. RF cavities for the Large Electron-Positron Accelerator [37] used electropolished copper as a substrate for niobium films deposited by magnetron sputtering, where the substrate conditions played a role in the eventual film purity and superconducting properties. New approaches using cathodic arcs [38] or high-impulse magnetron sputtering [39] coupled with copper or aluminum cavities processed by XMP could be interesting for cost savings due to the replacement of

substantial amounts of niobium with cheaper metal. Other approaches using vapor deposition [40] become quite interesting if given a starting surface that is already very smooth.

7. Conclusions

This paper described how an extended mechanical polishing technique resulted in dramatic improvement of surface finish and excellent superconducting properties in repaired SRF cavities used in particle accelerators. The mechanical polishing methods were developed by extending previous centrifugal barrel polishing techniques to fine polishing, where a special machine, tooling, and media produced action more akin to that of metallographic sample preparation on the inner surface of cavities. Mirror-smooth finishes were achieved, with an average surface roughness of 14 nm over a 1 mm profilometer scan. This is one order of magnitude lower in roughness than the typical finish produced by electropolishing, which is the present technique of preference for SRF cavities.

Weld pits could be removed and high accelerating gradients restored to affected cells by the XMP process. Replacement of bulk EP by XMP might therefore result in higher yield and lower cost for an industrial process to make SRF cavities for particle accelerators. Excellent performance was obtained after light electropolishing was subsequently applied to remove 20 μm of metal, even though this degraded the finish. Application of the XMP techniques to 9-cell cavities was successful, and the resulting facility did not require complicated safeguards for toxic chemicals or specialized protective gear.
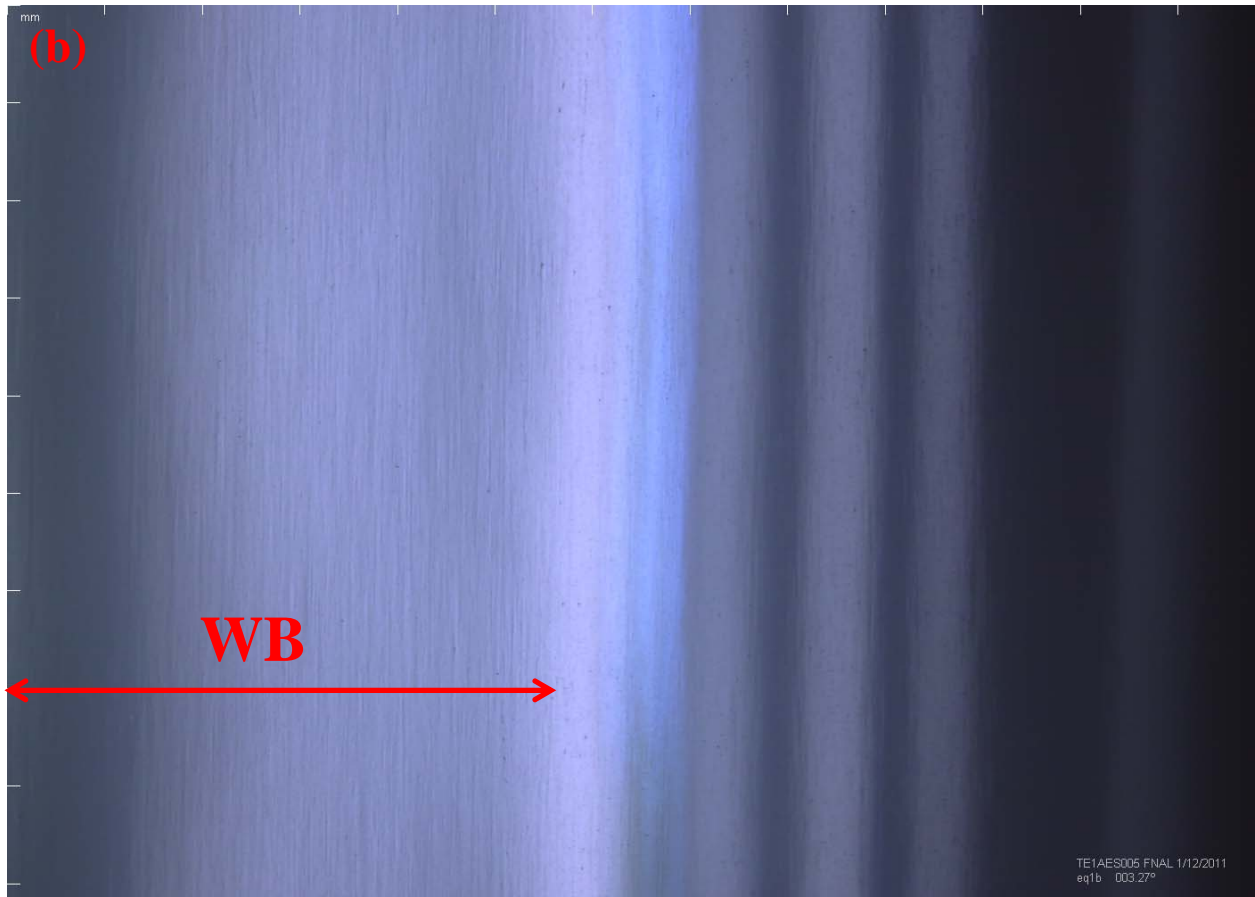
Acknowledgments

References

[1] Henning W and Schank C, *Acclerators for America's Future,* Report of the U.S. Dept. of Energy Workshop www.acceleratorsamerica.org/files/Report.pdf.
[2] Padamsee H, 2008 *RF Superconductivity* Vol. II *Science, Technology and Applications* (Weinheim: Wiley-VCH).
[3] Saito K, Inoue H, Kako E, Fujino T, Noguchi S, Ono M and Shishido T, 1998 *Part. Accel.* **60** 193.
[4] Tian H, Ribeill G, Xu C, Reece CE, and Kelley MJ 2011 *Appl. Surf. Sci.* **257** 4781.
[5] Hopkins JR and Finnemore DK 1974 *Physical Review B* **9** 108.
[6] Transtrum MK, Catelani G, and Sethna JP 2011 *Phys Rev. B* **83** 094505.
[7] Knobloch J, Geng R L, Liepe M, and Padamsee H, 1999 *Proc. 9th Workshop on RF Superconductivity* Santa Fe, NM, USA (published online at http://laacg.lanl. gov/rfsc99/rfsc99_web/TUA/tua004.pdf) 77
[8] Vines J, Xie, Y, and Padamsee H 2007 *Proc. 13th International Conf. RF Supercond.* Beijing, China (published online at http://accelconf.web.cern.ch/AccelConf /SRF2007/papers/tup27.pdf
[9] [Ciovati2007]
[10] [Romanenko2010]
[11] Koch C C, Scarbrough J O, and Kroeger D M 1974 *Phys. Rev. B* **9** 888.
[12] Halbritter J 1987 *Appl. Phys. A* **43** 1; Halbritter J, Kneisel P, Palmieri V, and Pekeler M 2001 *IEEE Trans. Appl. Supercond.* **11** 1864.
[13] Romanenko A and Padamsee H, 2010 *Supercond. Sci. Technol.* **23** 045008.
[14] Ciovati G, Kneisel P, and Gurevich A, 2007 *Phys. Rev. Special Topics Accel. Beams* **10** 062002.
[15] Dzyuba A, Romanenko A, and Cooley L D, 2010 *Supercond. Sci. Technol.* **23** 125011.

[16] Lilje L *et al*, 2004 *Nucl. Instrum. Methods Phys. Res.* A **524** 21.

[17] Zhao X *et al.,* 2010 *Phys. Rev. Special Topics Accel. Beams* **13** 124702.

[18] Tian H and Reece C E, 2010 *Phys. Rev. Special Topics Accel. Beams* **13** 083502.

[19] Cooley L D et al., 2011 *IEEE Tran. Appl. Supercond.* **21**, 3, 2609.

[20] [Tian]

[21] [Enzo-EP study]

[22] Higuchi T *et al.*, 1995 *Proc. 7th Workshop on Superconductivity* (Saclay, Gif sur Yvette, France) p. 723.

[23] Issarovitch G, Proch D, Singer X, Reschke D, and Singer W 2003 *Proc. 11th Workshop RF Supercond.* Lübeck/Tavemünder, Germany, p.482 (published online http://accelconf.web.cern.ch/accelconf /SRF2003/papers/tup56.pdf)

[24] Cooper C *et al.* 2009 *Proc. of SRF2009, Berlin, Germany* 806-10 (published online at http://accelconf.web.cern.ch/AccelConf/SRF2009 papers/tuppo076.pdf)

[25] [replicas]

[26] Iwashita Y, Tajima T and Hayano H 2008 Phys. Rev. Special Topics—Accel. Beams **11** 093501.

[27] [Samuels]

[28] Geng R L et al., 15th International Conference on RF Superconductivity (SRF 2011), Chicago, July 25-29, TUPO029.

[29] 1.3 Theoretical Limit

[30] Q-disease

[31] ILC Reference Design

[32] Kitamura

[33] Single grain cavity results

[34] Ricket

[35] IIT

[36] Wu

[37] LEP CAVITIES

[38] KRISH

[39] ANDERS

[40] PROLIER, CVD
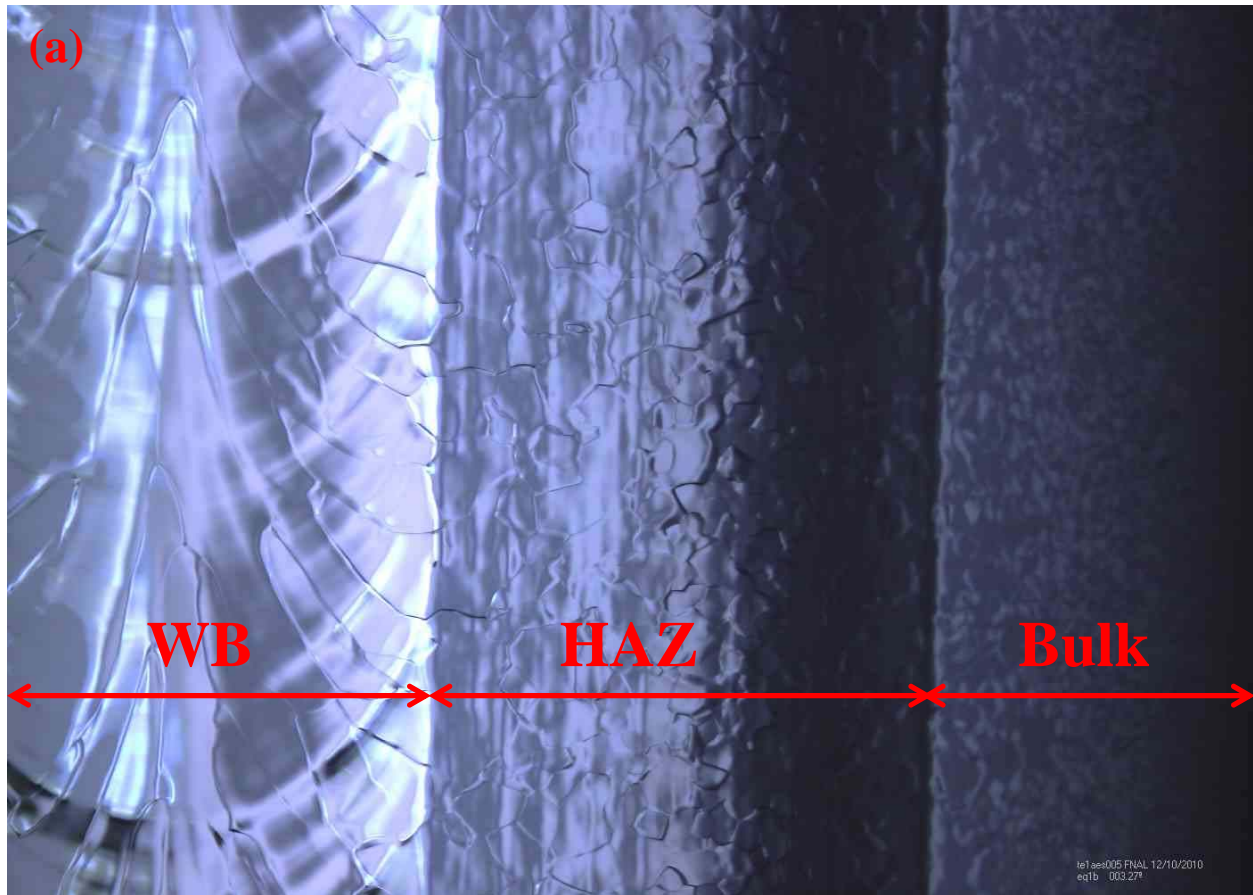
**Figure 1(a).** Figures 1(a), 1(b) and 1(c) are of equatorial weld beads under different processing conditions acquired by a cavity imaging system. In all pictures, WB indicates the extent of the weld bead, HAZ indicates the heat-affected zone, and Bulk refers roughly to unaffected niobium. During the process of weld preparation, some machining takes place to produce the vertical boundaries seen. Figure 1(a) shows TE1AES005 after standard electropolishing. This image is representative of what is seen on many other cavities after a standard EP process.

Figure 1(b) shows the same area in (a) after extended mechanical polishing to a mirror finish.
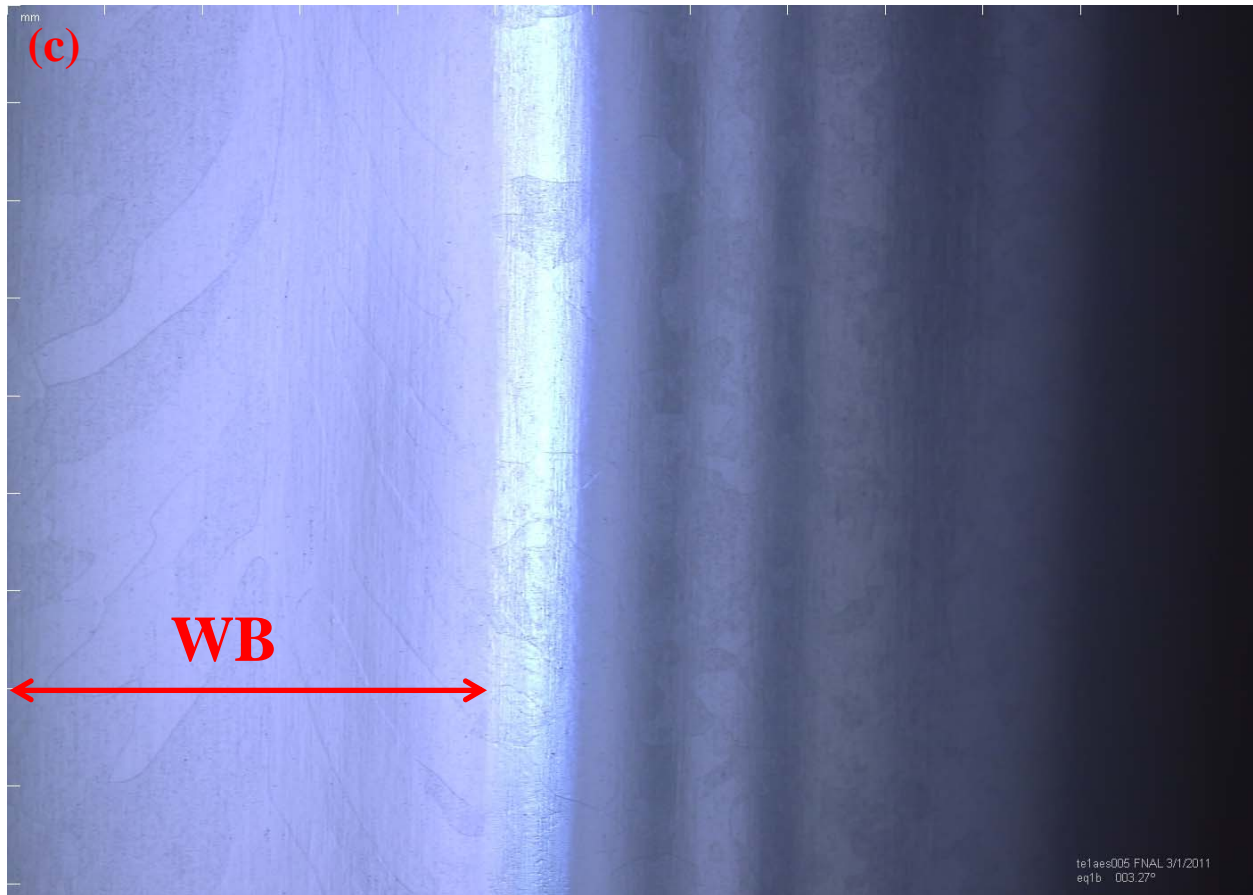
**Figure 1(c)** shows the same area seen in (b) after 10 µm of electropolishing.

Figure 1. Pictures of equatorial weld beads under different processing conditions acquired by a cavity imaging system. In all pictures, WB indicates the extent of the weld bead, HAZ indicates the heat-affected zone, and Bulk refers roughly to unaffected niobium. During the process of weld preparation, some machining takes place to produce the vertical boundaries seen. Figure 1(a) shows TE1AES005 after standard electropolishing. This image is representative of what is seen on many other cavities after a standard EP process. Figure 1(b) shows the same area in (a) after extended mechanical polishing to a mirror finish. Figure 1(c) shows the same area seen in (b) after 10 µm of electropolishing.

Figure 2(a). Pictures taken with a handheld digital camera of a single cell (a) and a nine cell (b) 1.3 GHz Tesla-type cavity after centrifugal barrel polishing to a mirror finish. The single cell cavity is standing on end on a piece of graph paper and the curved reflection of the grid can be seen in the cavity.
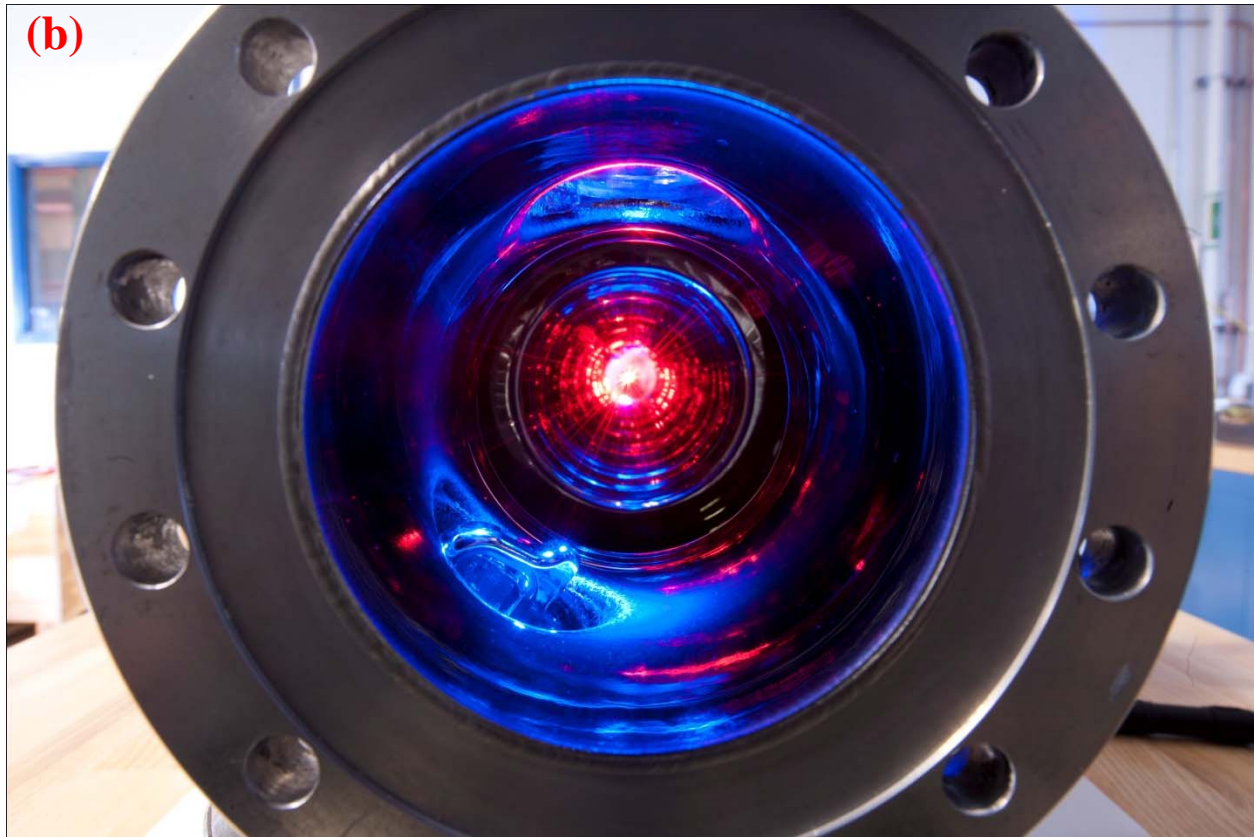
Figure 2(b). Picture taken of a 9-cell Tesla-type cavity after centrifugal barrel polishing to a mirror finish. Blue cellophane was placed over the light source to cut down on glare and a red light source was shown through the opposite end.
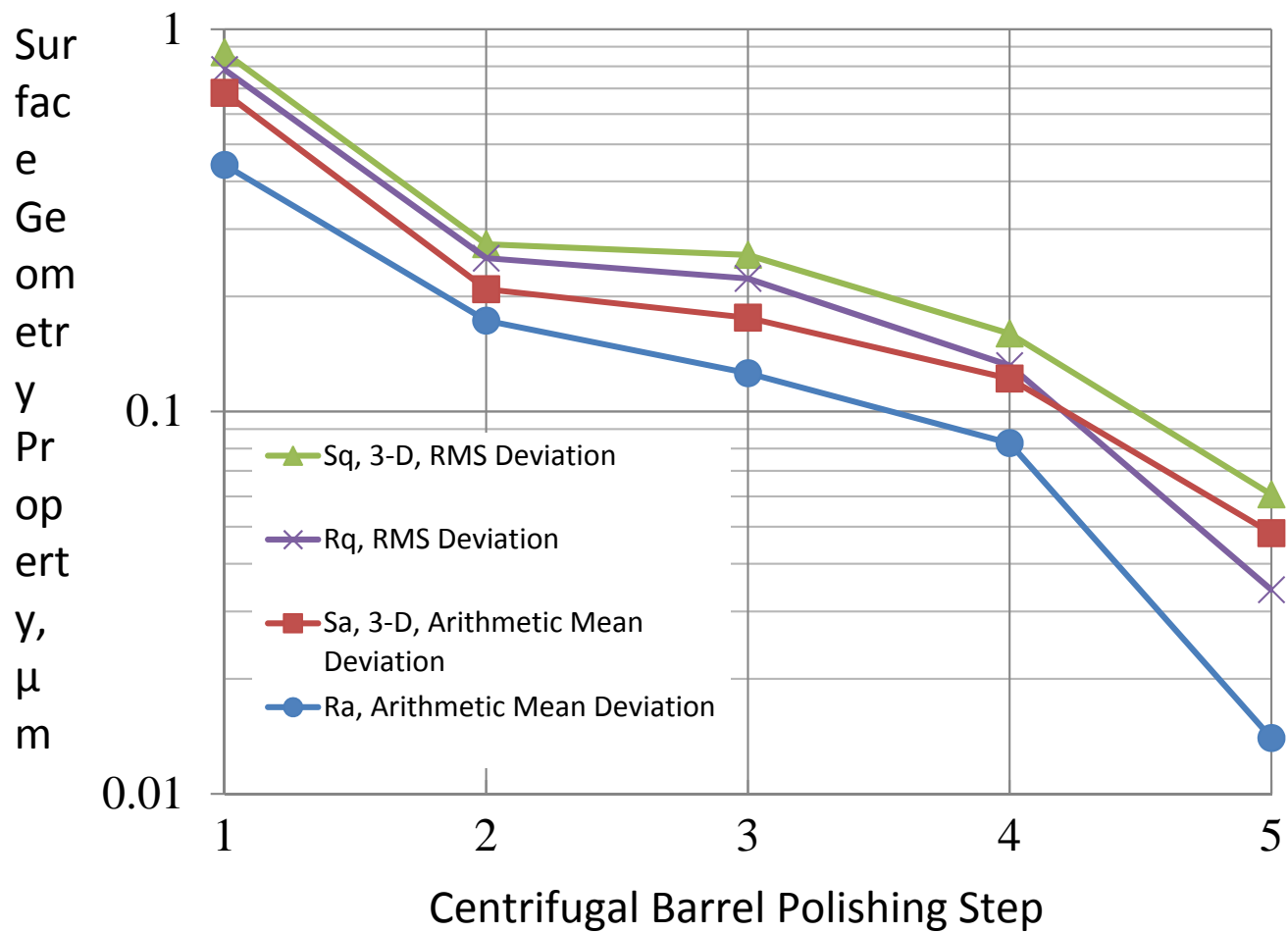
Figure 3. Is a graph of the RMS deviation and arithmetic mean data obtained from the surface profilometer after centrifugal barrel polishing with each one of 5 different media. Sample size is 1 mm with scans taken 1 micron apart and data points take every micron.
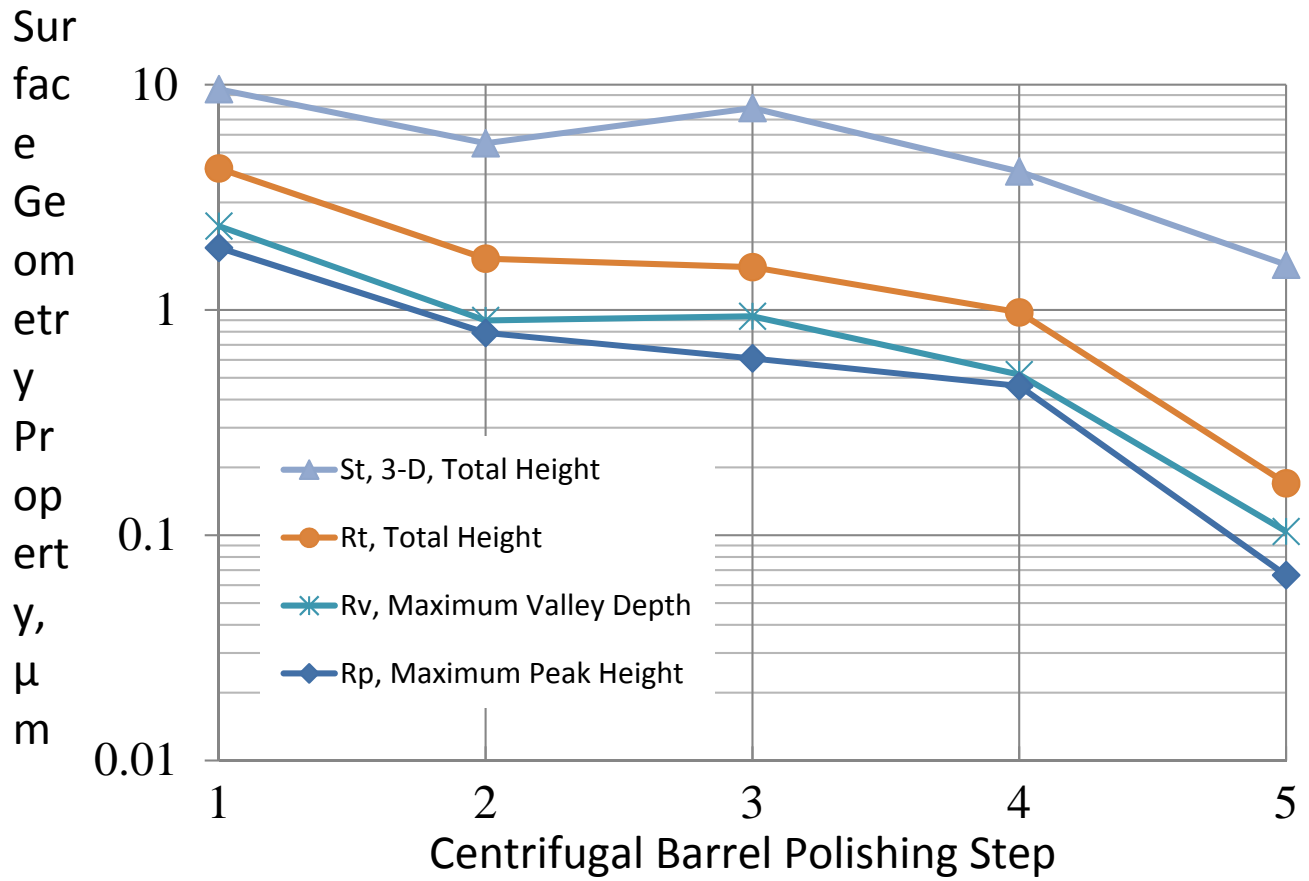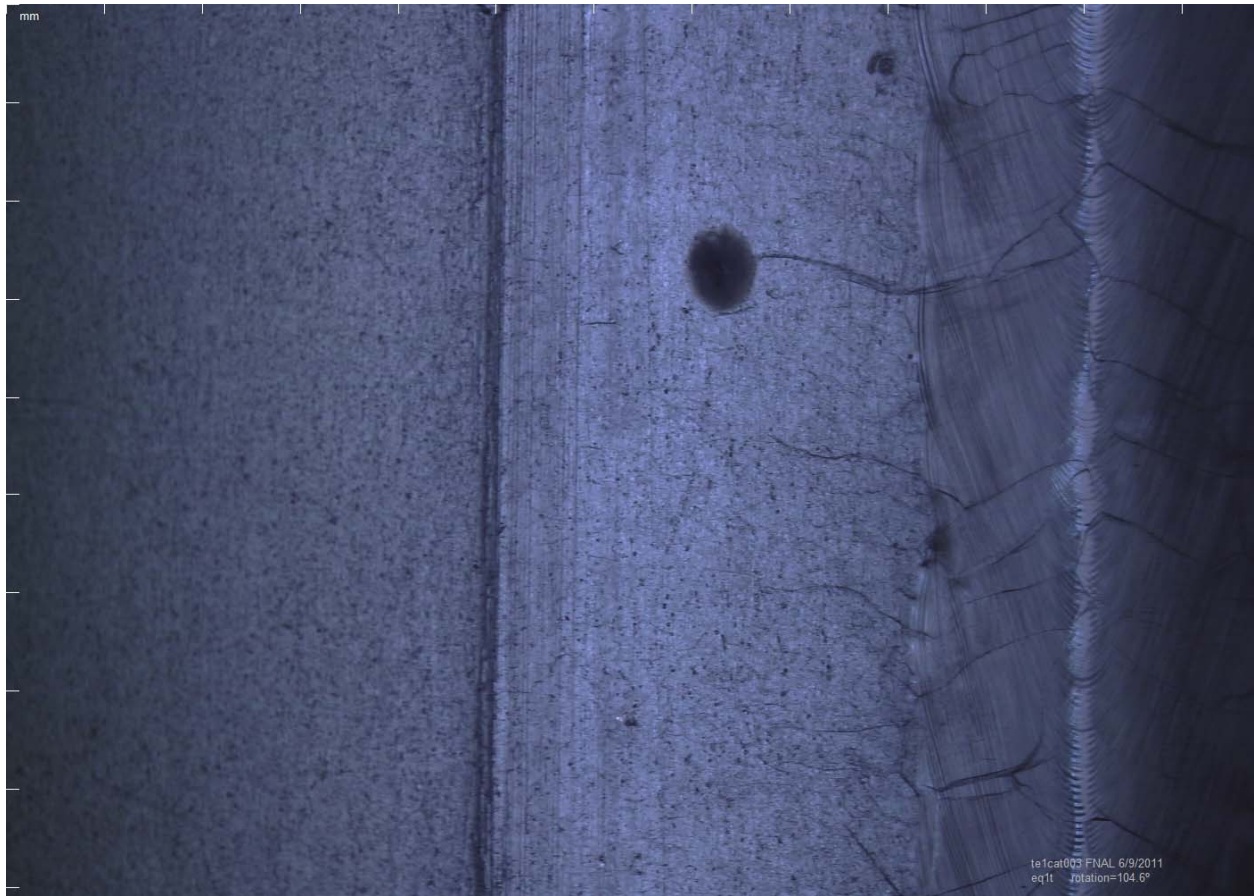
Figure 4. Is a graph of the maximum peak height and valley depth obtained from the surface profilometer after centrifugal barrel polishing with each one of 5 different media. Sample size is 1 mm with scans taken 1 micron apart and data points take every micron.
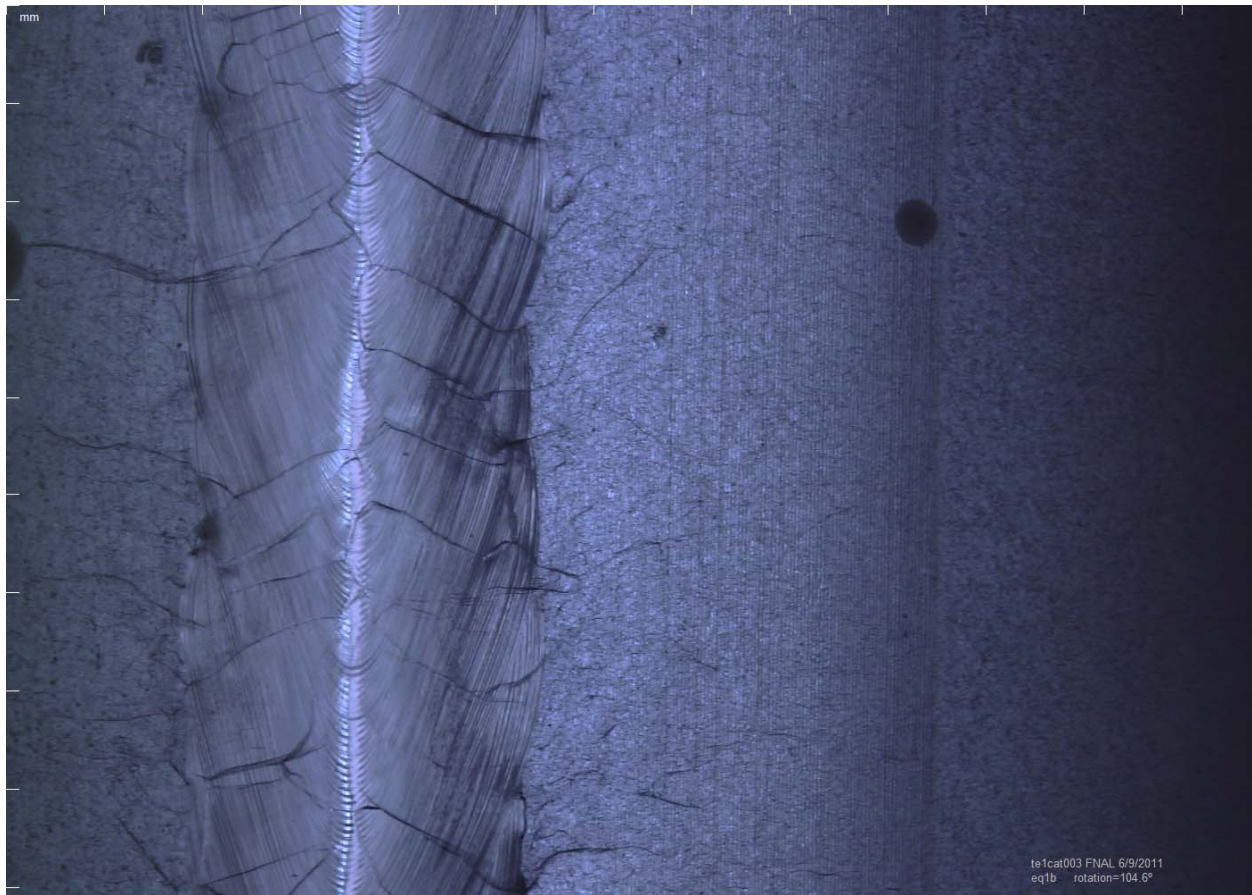
Figure 5 shows pictures of the equator electron bean weld area of single cell cavity RRCAT003. The large black dot is believed to be an inclusion, possibly of aluminum. Figure 5(a) shows a defective spot on the cavity after manufacturing. Figure 5(b) shows the cavity at the same spot after the baseline electropolishing technique. Figure 5(c) shows a different spot on the same cavity after manufacturing. Figure 5(d) shows the same area seen in 5(c) but after the baseline processing technique. Figure 5(e) shows the cavity after the XMP process. The picture shown in Figure 5(e) is at the same spot as the defect seen in Figure 5(a), but it is representative of the entire weld.
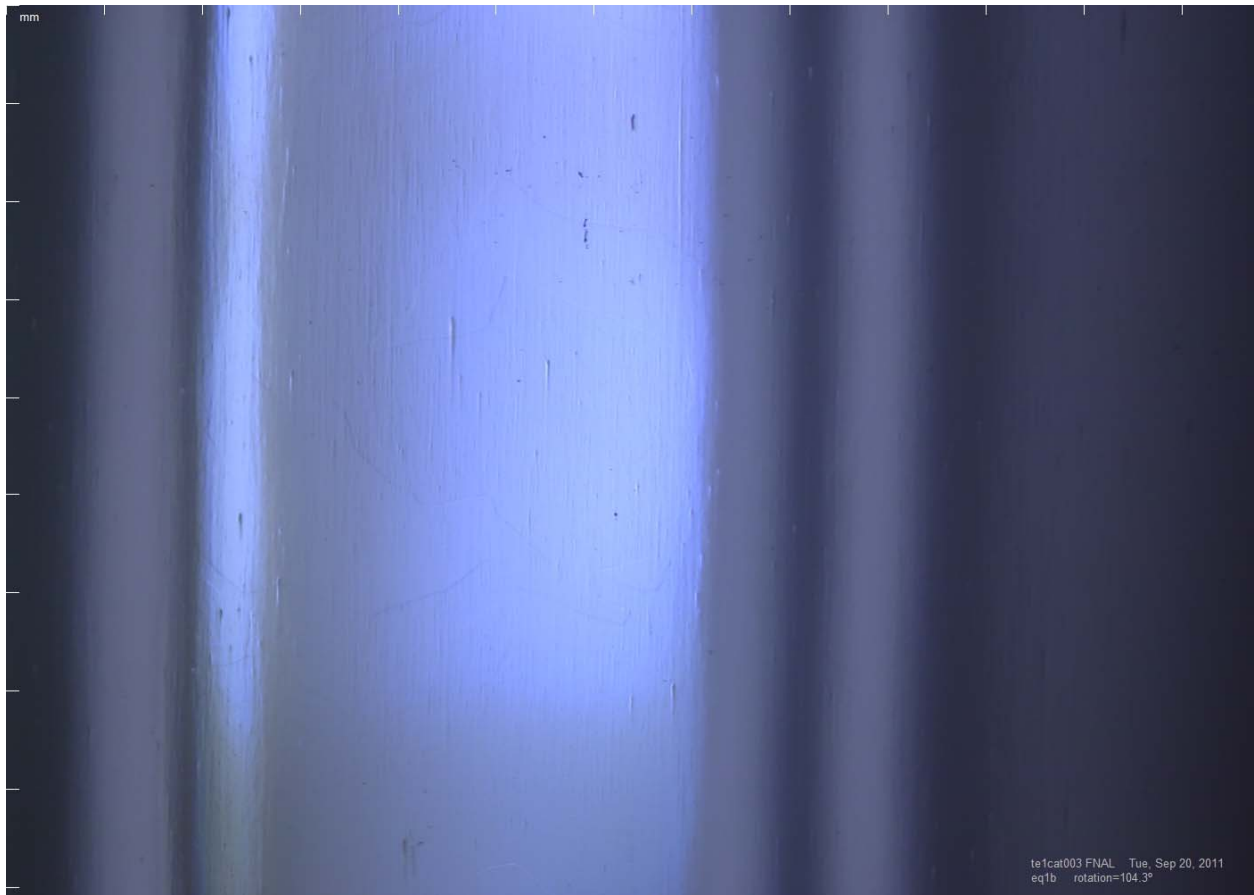
mm

te1cat003 FNAL   Mon, Aug 08, 2011
eq1b   rotation=104.6°

Figure 5(b) shows the cavity at the same spot after the baseline electropolishing technique.

Figure 5(c) shows a different spot on the same cavity after manufacturing.

Figure 5(d) shows the same area seen in 5(c) but after the baseline processing technique.

Figure 5(e) shows the cavity after the XMP process. The picture shown in Figure 5(e) is at the same spot as the defect seen in Figure 5(a), and is representative of the entire weld.
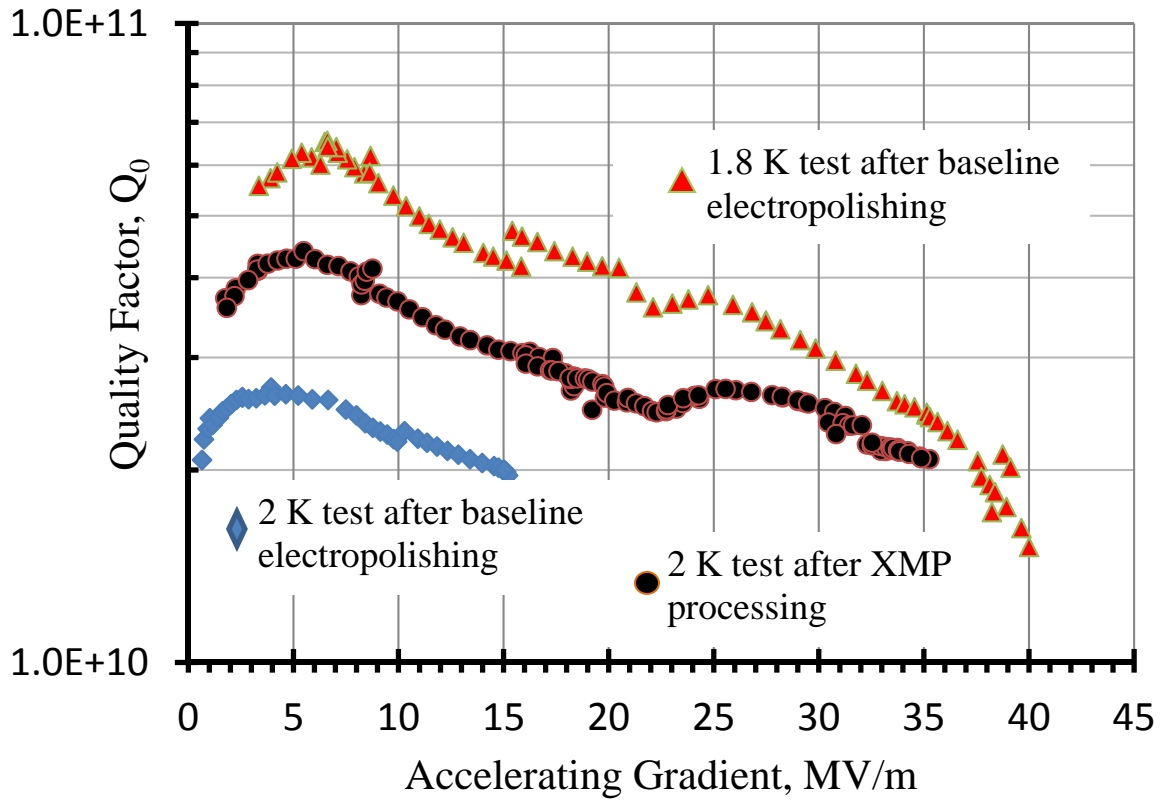
Figure 6 shows the accelerating gradient in MV/m versus the quality factor for single cell 1.3 GHz cavity RRCAT003 after baseline electropolishing (blue diamonds) and after XMP (black circles). Both tests are at 2 K. The red triangles are the results of the cavity after XMP and tested at 1.8 K.

Figure 7(a) shows a picture of the weld area of cavity TB9ACC015. There appears to be a large inclusion that was not removed by the standard electropolishing process.
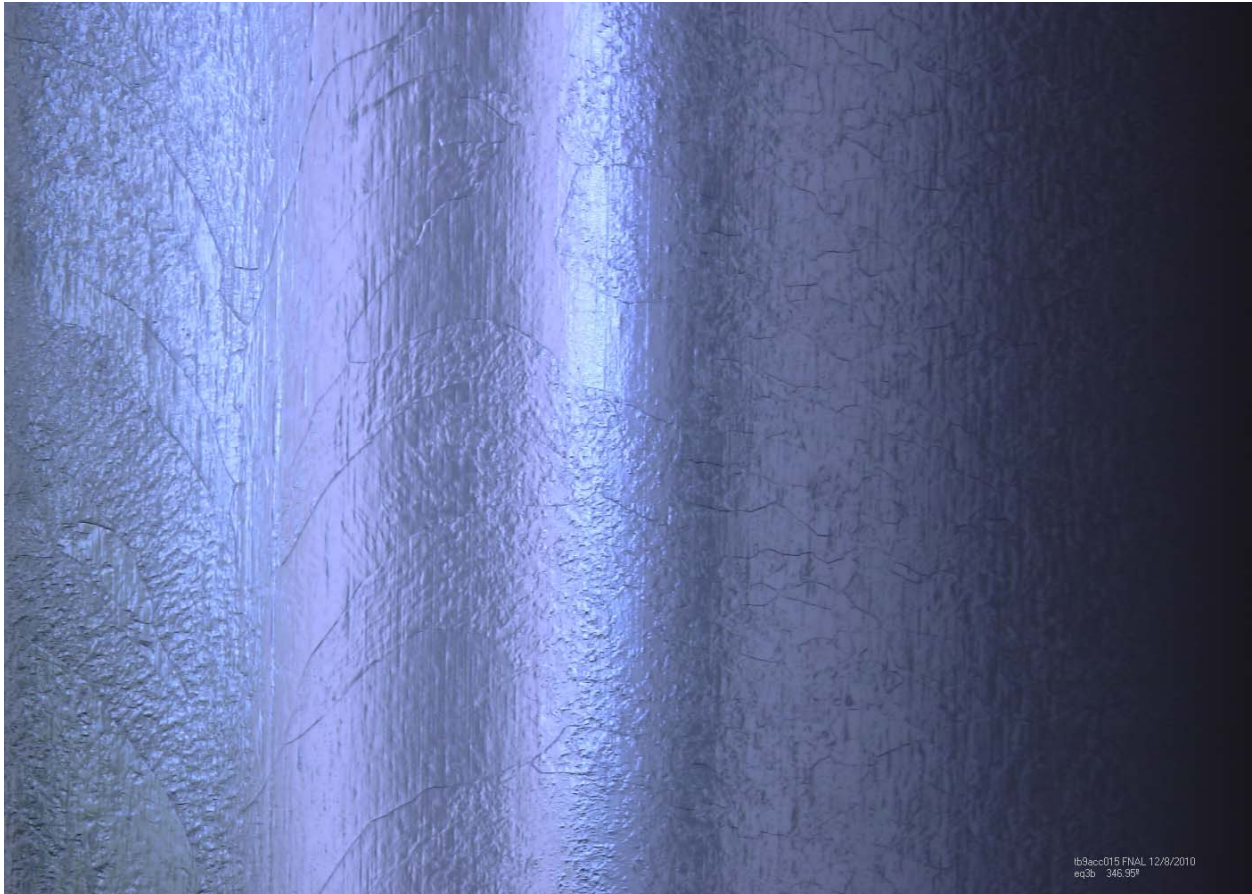
Figure 7(b) shows the same area as seen in Figure 7(a) but after centrifugal barrel polishing to an intermediate finish followed by a 60 micron electropolish. No sign of the defect remains.
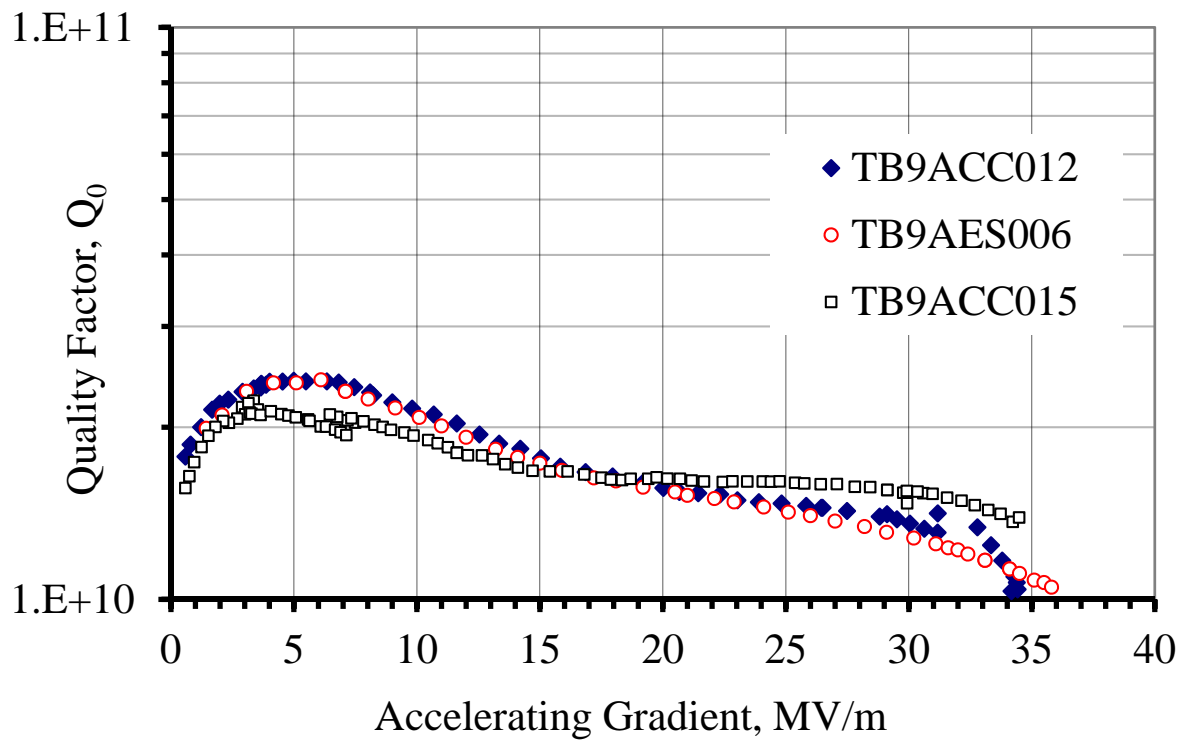
Figure 8 shows the 2 K performance results of various 9-cell cavities repaired by XMP. TB9AES006 and TB9ACC015 both had large defects and only performed at 19 MV/m before processing via XMP. TB9ACC012 was processed via electropolishing and then had the last 1 and ½ cells and end group replaced before processing before XMP. When testing under different Pi modes all cells in TB9ACC012 tested between 39 to 41 MV/m except the 2/8 cells due to the repair technique prior to XMP.
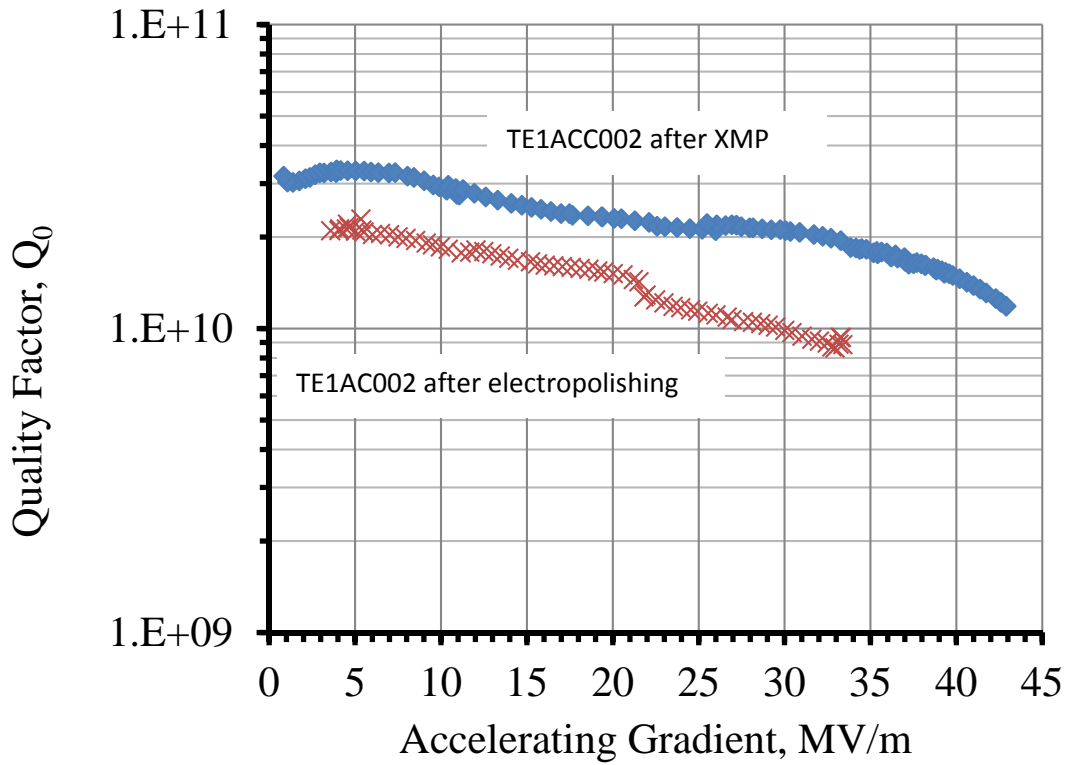
Figure 9 shows the improvement in performance data of single cell cavity TE1ACC002 in the form of accelerating gradient versus quality factor for the cavity after baseline processing with electropolishing (below) and after XMP (above). Tests were done at 2 K.
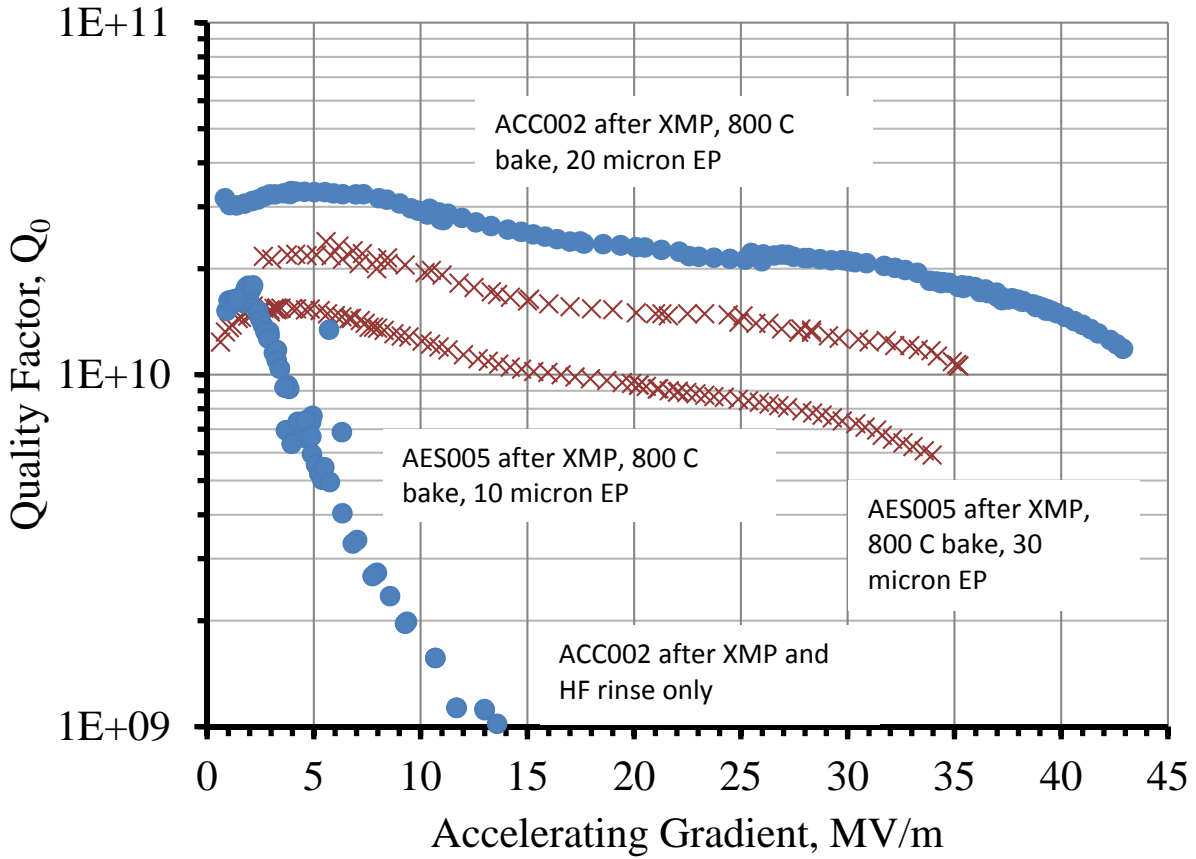
Figure 10 shows the 2 K quality factor versus accelerating gradient data for two different single cell cavities with varying amounts of post XMP chemistry. Both are single cell cavities that were polished to a mirror finish by XMP. The data shows that after 20 microns of chemistry the damage layer left from XMP is removed.